



**EFRE 2020**

# Formation of Double Shell During Implosion of Plasma Metal Puff Z-Pinches

Dmitry L. Shmelev

*Institute of Electrophysics, UB,  
RAS Ekaterinburg, Russia*

Alexander S. Zhigalin

*Institute of High Current  
Electronics, SB, RAS  
Tomsk, Russia*

Stanislav A. Chaikovsky

*Institute of Electrophysics, UB,  
RAS Ekaterinburg, Russia*

Vladimir I. Oreshkin  
*Institute of High Current  
Electronics, SB, RAS  
Tomsk, Russia*

Alexander G. Rousskikh  
*Institute of High Current  
Electronics, SB, RAS  
Tomsk, Russia*

**Abstract** — This work presents the results of experimental and theoretical research of impact of tailored density profile and application of external axial magnetic field on its implosion dynamics. It has been discovered that upon implosion of the plasma metal puff Z-pinch some stripes interpreted as the system of two coaxial shells appear on the optical images. With the help of numerical simulation, the formation of the plasma liner consisting of a mixture of carbon and bismuth ions has been considered. It has been shown that the lightweight carbon ions facilitate formation of the density distribution smoothly decreasing with the increase in radius, that, in turn, leads to suppression of the Rayleigh–Taylor instability in the current sheath upon further implosion. It has also been demonstrated that availability of the two types of ions in plasma considerably different in mass leads to formation of a double shell with externally located heavy ions. It has also been revealed that the application of the external axial magnetic field leads to reduction in the plasma metal puff Z-pinch initial diameter.

# Introduction

The fast Z-pinches are quite widely researched presently both in terms of their application as powerful source of soft X-ray radiation and regarding their possible use for inertial nuclear fusion [1-4]. The compression of the cylindrical fast Z-pinches takes place under the effect of a powerful current pulse creating high pressure of the magnetic field on the pinches external surface. In the presence of the magnetic fields the plasma compression is subject to magnetohydrodynamic instabilities. The most dangerous of which are Rayleigh–Taylor (RT) instabilities, that is why the fast Z-pinches implosion stabilization is one of the most important aspects of their physics [1,5-7]. To improve implosion stability different approaches were proposed and implemented, particularly, using of axial magnetic field and snow-plow stabilization mechanism.

The effective way to suppress the RT instabilities in Z-pinches can be the use of initial radial distribution of the substance density (tailored density profile [5]) at which the boundary between the magnetic field and plasma is not exposed to acceleration and the exponential growth of RT instability is suppressed. To suppress the RT instabilities the authors of the work [5] proposed to use such an initial distribution of the substance in the shell at which the density decreases according to the law  $\rho(R) \sim R^{-s}$ , where  $s > 2$ . Upon compression of the substance with such density distribution the plasma boundary velocity begins to decrease after a short period of initial growth. One more consequence of the use of this kind of a profile is emergence of the low-density plasma on the periphery of the pinch. Ions with different charge-to-mass ratios can be separated in such plasma. This can be seen in the plasma consisting of a mixture of substances.

Tailored density profile was implemented in the experiments on the plasma metal puff Z-pinch implosion [8-10]. The metal puff Z-pinches are formed by injecting high-current vacuum arc plasma into a vacuum gap, the electrodes of which are under the voltage supplied by a generator with the current amplitude about a megampere to produce the z-pinch. It was shown [9] that the energy radiated from the Z-pinch can be considerably changed with the help of external axial magnetic field, the induction of which is much less than the induction of the Z-pinch self-magnetic field. It was demonstrated that the radiation energy of the bismuth Z-pinch compressed by IMRI-5 generator (450 kA, 450 ns) at  $B_{z0} = 4.5$  kGs is about one and a half times as powerful as the Z-pinch energy without external magnetic field. The dynamics of Z-pinch compression and the total radiation output are mainly determined by initial spatial distribution of plasma liner density in the interelectrode gap. The aim of this article is experimental and theoretical research of impact of tailored density profile and application of external axial magnetic field both on initial spatial distribution of the plasma density in the plasma metal puff Z-pinch and on its implosion dynamics.

# Experimental Setup

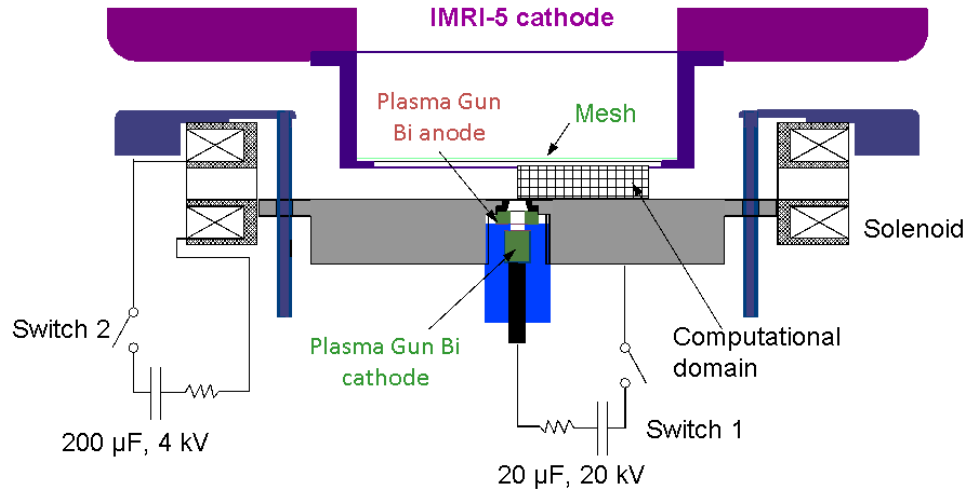


Fig.1 Geometry of the problem

The experiments have been carried out on the high-current IMRI-5 pulse generator [8-10] with the current amplitude of about 450 kA and a rise time of around 500 ns. The scheme of experiments is presented in Fig.1. The plasma produced by vacuum-arc discharge was used as the load of the generator. The electrodes of the plasma gun (both cathode and anode) were made from bismuth. The plasma jet was injected through a hole in the steel collimator, 5 mm in diameter. The length of the liner was 1 cm. It should be mentioned that the plasma injected from the plasma gun contained not only bismuth ions which the electrodes were made but also the ions of isolator substance (mainly carbon ions [11]). All the experiments on the metal puff Z-pinch compression were carried out under the following fixed conditions: the delay between the beginning of the current flow in the arc discharge and switching the IMRI-5 generator current (450 kA, 450 ns [9]) was  $\Delta t_{pl}=6.2 \mu s$ ; the voltage of the capacitor charging ( $C_{pl}=20 \mu F$ ) of the plasma source  $U_{pl}=20 kV$ ; a quarter of the current oscillation period in the arc discharge was  $t_{1/4}=6.67 \mu s$ , arc discharge current was  $92 \pm 2 kA$ . Fixing of these conditions provided similar initial linear mass of the liners. It should, however, be mentioned that the application of the external magnetic field (see below) affected the plasma gun functioning, that, in turn, influenced the initial substance distribution in the interelectrode gap of IMRI-5 generator.

# Experimental procedure

The external magnetic field was produced with the help of the two coils connected in series (Fig.1). Each coil had 60 spirals. The capacitance in the magnetic field generation system was  $C_{bf}=200 \mu\text{F}$ . The charge voltage of the system was  $U_{bf}=4 \text{ kV}$ . The value of the magnetic field at the moment of switching on of the plasma source (and then IMRI-5 generator) was varied by changing the time interval  $\Delta t_{bf}$  between the beginning of the current flow in the magnetic field coil and the time of switching the rest of the system. The experiments were carried out at the following parameters of the magnetic field:  $B_1=1.5 \text{ kGs}$  ( $\Delta t_{bf}=47 \mu\text{s}$ );  $B_2=3 \text{ kGs}$  ( $\Delta t_{bf}=114 \mu\text{s}$ );  $B_3=4.5 \text{ kGs}$  ( $\Delta t_{bf}=200 \mu\text{s}$ );  $B_4=6 \text{ kGs}$  ( $\Delta t_{bf}=360 \mu\text{s}$ ).

The diagnostics during the experiments included both current and voltage measurements and registration of the images of the liners in their self-radiation. To obtain the plasma images in the visible spectral range the HSFC Pro four-frame optical camera with the exposure of 3 ns was used. Besides, current sheath boundary position upon the plasma pinch compression was determined during the experiments; detailed description of the measurement techniques is given in the paper [10].

In the series of the experiments describes in [10], the current sheath boundary position upon the plasma liner compression was determined using three different methods: by magnetic probe, by optical observation and by measurement of the inductance  $L(t)$  according to the following formula:

$$R(t) = R_r \exp\left[-\frac{L(t) - L_0}{2}\right] \quad (1)$$

where  $R(t)$  – sheath radius,  $R_r$  –reverse current posts radius,  $L_0$  – the inductance of the circuit section between the voltage gauge position and the Z-pinch. The all three measurement methods showed comparable results [10].

# Experimental procedure

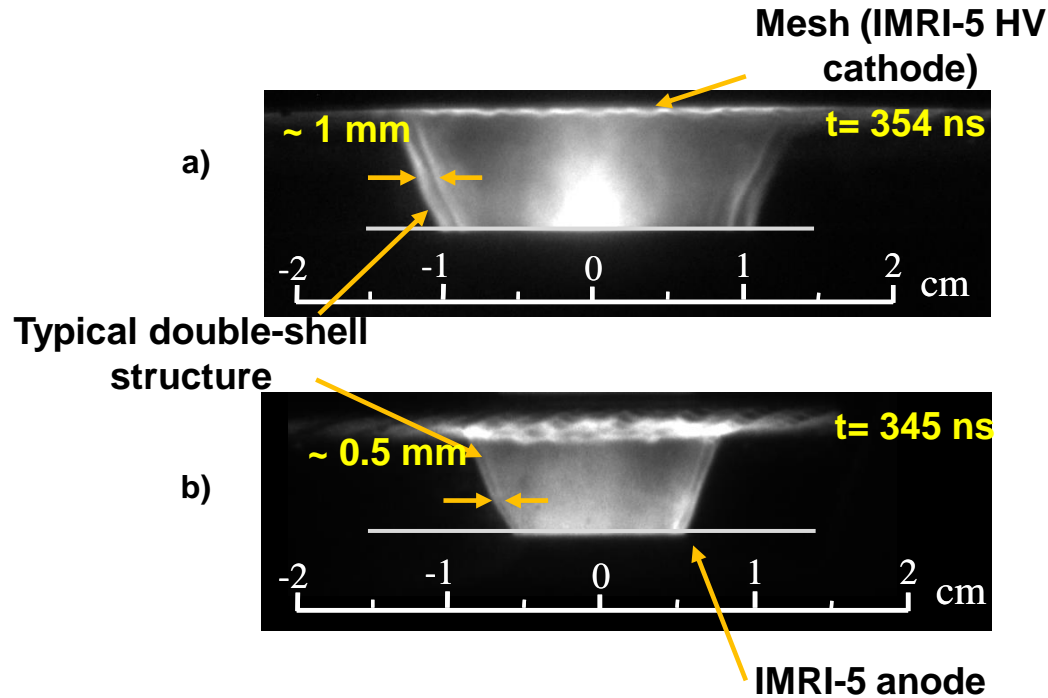


Fig.2 Two parallel glowing shells observed during the experiment. a) Shot at  $B_z = 0$ . b) Shot at  $B_z = 3$ . kGs

The pictures of the self-emission of the Z-pinchs taken with the help of HSFC Pro optical camera revealed that there were the stripes parallel to the direction of the current flowing through the pinch (Fig.2) on some images. The stripes were logical to associate with a system of two coaxial shells. These stripes or shells were the most clearly displayed when the pinch radius was approaching the value of about 1 cm and the distance between the stripes was around 1 mm. And this type of structure could be seen both in the absence and in the presence of the external magnetic field (Fig.2). The nature and mechanism of emergence of the above structure we attempted to figure out with the help of numerical simulation.

# Numerical model brief description

For simulation of the vacuum arc plasma jet expansion and the subsequent Z-pinch implosion the two-dimensional hybrid model of quasi-neutral plasma was developed and tested [12-14]. The model considers the all three components of ion and electron velocities, current and magnetic field, but all the components depend only on the two variables -  $r$  and  $z$ . This modification of the model allows researching the impact of the external axial magnetic field on the metal puff Z-pinch dynamics. The applicability of this code for the Z-pinch compression related problems was tested in [14]. Here we will give only brief description of the model.

The model is a hybrid one., i.e. the ions are treated as the macroparticles with the help of the particles-in-cells (PIC) method. The macroparticles can describe the particles of different type, i.e. the particles having different charge and mass. The electrons are treated as the massless fluid in the framework of quasineutrality. Direct ionization, triple recombination, photo recombination were considered. The reactions were simulated with the help of direct simulation Monte Carlo method. The radiation losses were calculated in course of computation of radiation transfer with the use of P1 method. The problem was solved in cylindrical geometry on rectangular grid. The size of the computational domain (Fig. 1): radius – 3,25 cm, height – 1 cm. The size of the computational cell of the grid varied upon the increase in the radius from  $25 \mu\text{m} \times 50 \mu\text{m}$  to  $90 \mu\text{m} \times 50 \mu\text{m}$ .

During calculations, we tried to obtain such a plasma distribution in the gap that, upon compression of the liner, would create a current pulse reproducing the  $R(t)$  curve obtained during the experiment. The  $R(t)$  was understood as a medium current sheath radius which, as in the experiment, was calculated according to the formula (1). The fit to the experimental pinch compression curve was carried out in the absence of the external axial magnetic field. The boundary conditions for the plasma jet flowing from the vacuum-arc plasma source, obtained as a result of the above fitting remained unchanged in the computation of the plasma expansion in the external magnetic field.

# Results of calculations

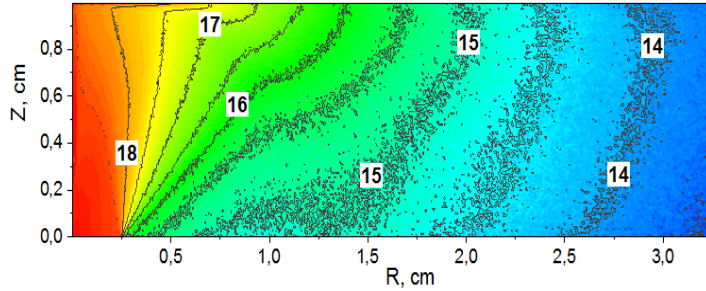


**Fig.3** Aggregated (C+Bi) ions density ( $\lg(n)$ ,  $n$  ( $\text{cm}^3$ )).  $B_z = 0$ .

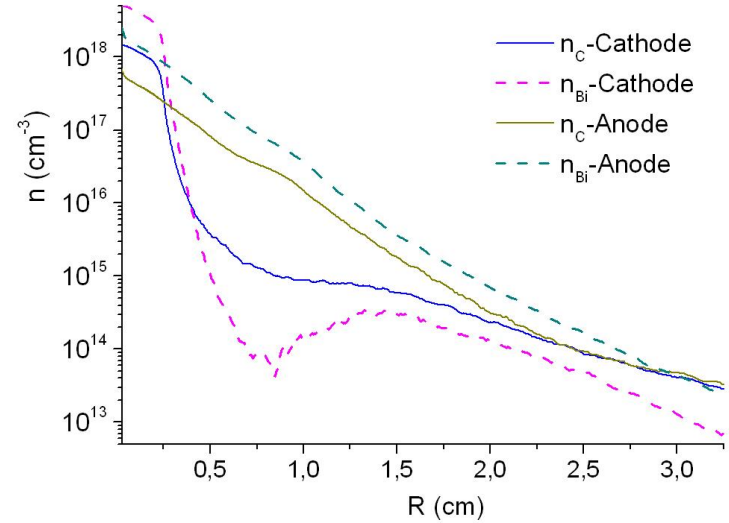


**Fig.4** Distribution of different component ions density in the gap.  $B_z = 0$ .

The ions density distribution in the interelectrode gap at zero axial magnetic field is presented in Fig. 3, 4. It is seen that the density distribution in the gap has a profile smoothly decreasing with an increase of  $R$ . In the center of the gap at  $R > 0.25$  cm the density behaves as follows:

$$n(R) = 10^{18} e^{-(3.5R)^2} + 3 \cdot 10^{15} R^{-3.5}$$

i.e. in case of high radius values  $R > 0.7$  cm the condition of RT instability suppression [5] is met.

In Fig.4 one can see that such a profile (at high  $R$  values) is mainly formed by the carbon ions, and the bismuth ions create the central dense jet. It should be noted that a similar structure of the initial metal puff plasma  $Z$ -pinches substance distribution was observed in the experiments [11]. The distribution of bismuth and carbon ions in the anode is similar owing to a considerable number (25%) of the ions reflected from the grid which mix with the ions approaching the anode. Although the carbon ions are injected in a three times lower quantity, they make the distribution of the aggregated density along  $Z$  at higher  $R$  values more homogeneous that positively influences the consequent implosion dynamics.

## Results of calculations (2)

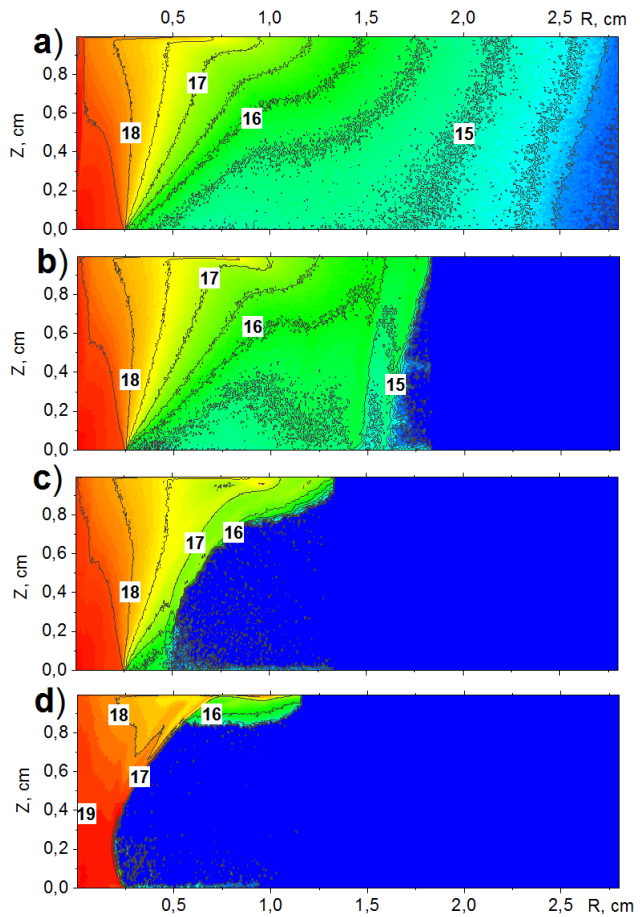


**Fig.5** Plasma liner compression.

Aggregated (C+Bi) ions density ( $\lg(n)$ ,  $n$  ( $\text{cm}^3$ )) at different points of time.  $B_z = 1.5$  kGs. a)  $t=10$  ns, b)  $t=200$  ns, c)  $t=300$  ns, d)  $t=350$  ns.

According to [5], the Z-pinch density profile subject to power law of density reduction suppresses the development of Rayleigh–Taylor instability during the implosion of the z-pinch that results in more homogeneous compression involving almost all substance of the pinch. In case of compression of a sharp boundary pinch, the Rayleigh–Taylor instabilities develop in the current sheath that makes only a part of the pinch substance to compress. As some experimental research [9, 10] reveal, the pinch formed by the above method is compressed homogeneously without any visible disturbances typical for the developed Rayleigh–Taylor instability. In our simulation the pinch also was compressed quite homogeneously without any instabilities in the current sheath (Fig. 5).

## Results of calculations (3)

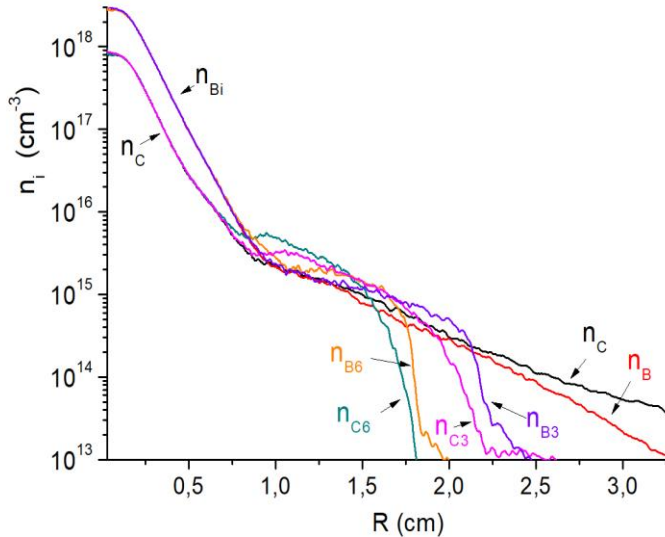
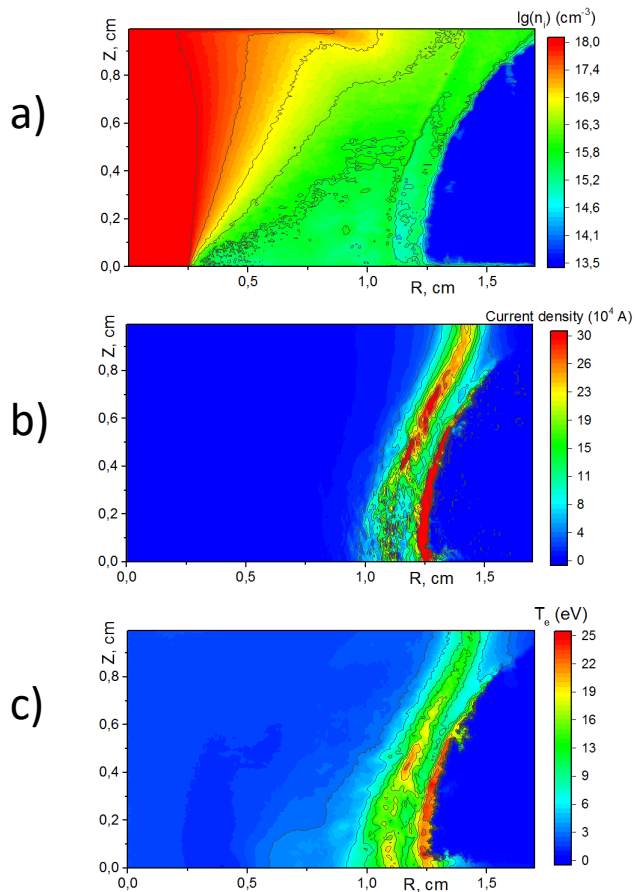


**Fig.6** Distribution of the ion densities at different external axial fields. “C” and “B” stand for carbon and bismuth. The numbers 0, 3, 6 mean that the computation was made at  $B_z=0, 3., 6.$  kGs respectively.

Fig. 6 shows the density distribution in the center of the gap obtained at different values of the external axial magnetic field. The plasma pinch initial radius decreases nonotonously with the increase in  $B_z0$ . It should be mentioned that during the computation it was assumed that the external magnetic field in the interelectrode gap was homogeneous at the beginning and had only Z-component. The actual axial magnetic field in the experimental installation is not homogeneous and has a nonzero R-component. But at this stage the task was simplified to discover main regularities of the external field influence.

One can see that if at  $B_{z0}=0$  the Bi ions density decreases with the radius faster than C ions density, than at  $B_{z0}>0$  there is the contrary situation. This is since the forces driven by the presence of gradients of the thermal pressure and the magnetic field in plasma have different impact on different substances ions. The carbon ions being more lightweight are faster decelerated by the magnetic field, and the ion-ion interaction is weak due to the low plasma density and is not able to equalize the different mass ions velocities.

## Results of calculations (4)



After the start of implosion the carbon ions are accelerated intensively than bismuth ions and the two parallel converging shells appear. Such shells can be seen in Fig. 5 b), Fig. 7, and Fig. 8 clearly demonstrate that such shells correspond to the local maxima of the different mass ions density which are also accompanied by the local maxima of the current density and electron temperature.

**Fig.7** a) Aggregated density of plasma ions ( $\lg(n)$ ,  $n$  ( $\text{cm}^3$ )); b) Current density; c) electron temperature.  $B_z=0$ ,  $t=230$  ns. Two parallel shells can be seen at the external boundary.

## Results of calculations (5)

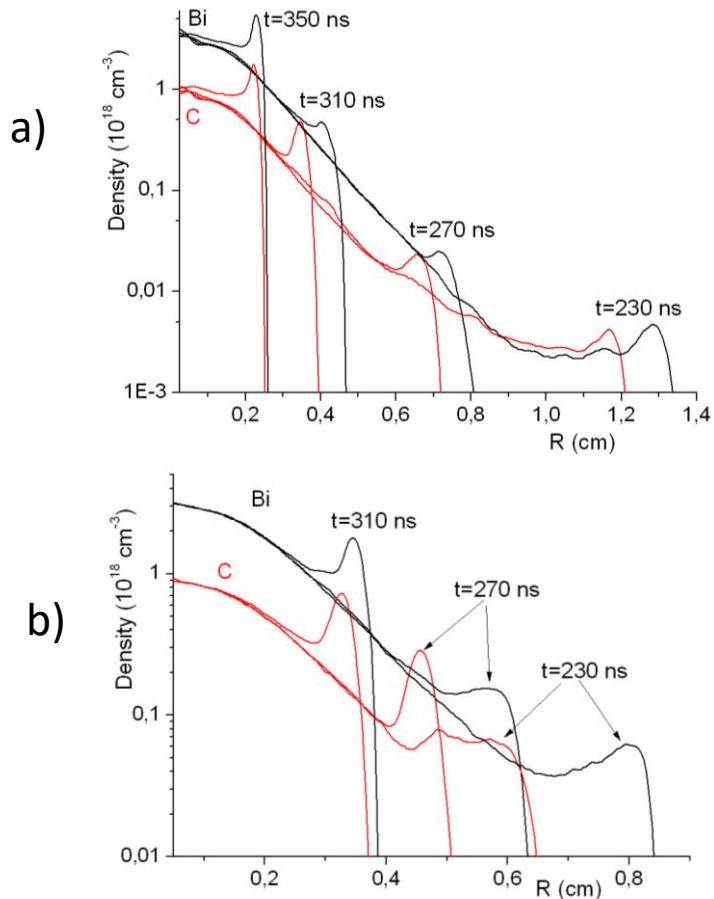


**Fig.8** Averaged ions densities distribution in the center of the gap at different points of time. a)  $B_z=0 \text{ kGs}$ ; b)  $B_z=3 \text{ kGs}$ .

The simulation has also revealed that the distance between the shell's changes during the pinch compression (Fig. 8). When the compression starts the distance increases – the carbon ions move forward. When the shells approach the dense plasma area the lightweight ions are decelerated more efficiently, the distance between the shells decreases. Upon the further compression of the pinch, i.e. when the shells enters the dense plasma area the efficiency of the ion-ion interaction enhances, the drift velocities of different mass ions equalize, and the two shells merge into one ( $t=350 \text{ ns}$ , Fig. 8a and  $t=310 \text{ ns}$ , Fig. 8b). This kind of double luminous shells which merge into one at a later point of time during the compression are observed during the experiments (Fig. 2).

## Conclusion

Thus, the work presents the results of experimental and theoretical research of impact of tailored density profile and external axial magnetic field on initial spatial distribution of the plasma metal puff Z-pinch and on its implosion dynamics. The experiments have revealed that upon implosion of the metal puff Z-pinch some stripes parallel to the direction of the current flowing through the liner appear on the optical images obtained in their self-emission. The stripes have been interpreted as the system of two coaxial shells. Such structure is observed when the compressing pinch radius value approaches 1 cm, and the “stripes” appear both in the absence and in the presence of the external magnetic field. The formation of the plasma pinch consisting of a mixture of carbon and bismuth ions as a result of the expansion of the arc plasma jet ignited on the bismuth electrode has been considered in the present study with the help of the numerical simulation. It has been revealed that the lightweight carbon ions facilitate generation of the tailored density profile which, in turn, provides suppression of the Rayleigh–Taylor instability in the current sheath upon the consequent implosion. It has also been demonstrated that availability of the two ion types considerably different in mass in the pinch plasma leads to formation of the double shells with externally located heavy ions in the compression phase. It has been shown that the application of the external axial magnetic field results in decrease in initial diameter of the plasma metal puff Z-pinch. The obtained results are in good agreement with the experimental data.

# REFERENCES

- [1] M.G. Haines, “A review of the dense Z-pinch”, *Plasma Phys. Control. Fus.* 2011. vol. 53. P. 093001.
- [2] B. Jones, C. Deeney, C.A. Coverdale, P.D. LePell, J.L. McKeeney, J.P. Apruzese, et al., “K-shell radiation physics in low-to moderate-atomic-number z-pinch plasmas on the Z accelerator”, *J. Quant. Spectrosc. Radiative Transfer*, 2006, vol.99, pp.341-348.
- [3] A.V. Branitskii, V.V. Aleksandrov, E.V. Grabovskii, V.V. Zazhivikhin, M.V. Zurin, S.F. Medovshchikov, et al., “Cold-start effects in experiments on the implosion of plasma liners in the Angara-5-1 facility”, *Plasma Physics Reports*, 1999, vol. 25, pp. 976-993.
- [4] S.A. Slutz, M. C. Herrmann, R.A. Vesey, A.B. Sefkow, D.B. Sinars, D.C. Rovang, et al., “Pulsed-power-driven cylindrical liner implosions of laser preheated fuel magnetized with an axial field” , *Phys. Plasmas*, 2010. V. 17. P. 056303.
- [5] A.L. Velikovich, F.L. Cochran, and J. Davis, “Suppression of Rayleigh-Taylor Instability in -Pinch Loads with Tailored Density Profiles”, *Phys. Rev. Lett.*, 1996, vol. 77, pp. 853-856.
- [6] R.B. Baksht, I.V. Datsko, and A.A. Kim, “Rayleigh-Taylor instability and K-radiation yield in compression of gaseous liners”, *Physica Plasmy (in Russian)*, 1995, vol. 21. pp. 959-965.
- [7] A.Yu. Labetsky, R.B. Baksht, V.I. Oreshkin, A.G. Rousskikh, and A.V. Shishlov, “An experimental study of the effect of Rayleigh-Taylor instabilities on the energy deposition into the plasma of a Z pinch”, *IEEE Trans. Plasma Sci.*, 2002, Vol. 30, pp. 524 – 531.
- [8] A.G. Rousskikh, A.S. Zhigalin, V.I. Oreshkin, N.A. Labetskaya, S.A. Chaikovsky, A.V. Batrakov, et al., “Study of the stability of Z-pinch implosions with different initial density profiles”, *Phys. Plasmas*, 2014, vol: 21, 052701.
- [9] A.G. Rousskikh, A.S. Zhigalin, V.I. Oreshkin, V. Frolova, A.L. Velikovich, G. Yu. Yushkov, and R. B. Baksht, “Effect of the axial magnetic field on a metallic gas-puff pinch implosion”, *Phys. Plasmas*, 2016, vol. 23, 063502.
- [10] A. G. Rousskikh, A. S. Zhigalin, V. I. Oreshkin, and R. B. Baksht, “Measuring the compression velocity of a Z pinch in an axial magnetic field”, *Phys. Plasmas*, 2017, vol. 24, 063519
- [11] A.G. Rousskikh, A.S. Zhigalin, and V.I. Oreshkin, “Estimation of the initial density distribution in plasma-metal liners”, *Technical Physics*, 2016, vol. 61, pp. 676-682.
- [12] D.L. Shmelev, I.V. Uimanov, “Hybrid computational model of high-current vacuum arcs with external axial magnetic field”, *IEEE Trans. Plasma Sci.*, 2015, vol. 43, pp. 2261-2266.
- [13] D.L. Shmelev, V.I. Oreshkin, and I.V. Uimanov, “Hybrid numerical simulation of high-current vacuum arc taking into account secondary plasma generation”, *IEEE Trans. Plasma Sci.*, 2019, vol. 47, pp. 3478- 3483.
- [14] D.L. Shmelev, V.I. Oreshkin, and S.A. Chaikovsky, “Hybrid MHD/PIC simulation of a metallic gas-puff Z-pinch implosion”, *Journal of Physics: Conf. Series*, 2018, vol. 1115, 022014